CrossMark

ORIGINAL PAPER

Characterization of nitrogen substrate limitation on *Escherichia coli*'s growth by parameter identification tools

M. Rios-Lozano[1] · V. Guerrero-Torres[1] · A. Badillo-Corona[2] · I. Chairez[2] ·
C. Garibay-Orijel[2]

Abstract Carbon-to-nitrogen ratio (CNR) has shown to be a relevant factor in microorganisms growth and metabolites production. It is usual that this factor compromises the productivity yield of different microorganisms. However, CNR has been rarely modeled and therefore the nature of its specific influence on metabolites production has not been understood clearly. This paper describes a parametric characterization of the CNR effect on the *Escherichia coli* metabolism. A set of parameters was proposed to introduce a mathematical model that considers the biomass, substrate and several byproducts dynamical behavior under batch regimen and CNR influence. Identification algorithm used to calculate the parameters considers a novel least mean square strategy that formalizes the CNR influence in *E. coli* metabolism. This scheme produced a step-by-step method that was suitable for obtaining the set of parameters that describes the model. This method was evaluated under two scenarios: (a) using the data from a set of numerical simulations where the model was tested under the presence of artificial noises and (b) the information obtained from a set of experiments under different CNR. In both cases, a leave-one-experiment-out cross-validation study was considered to evaluate the model prediction capabilities. Feasibility of the parametric identification method was proven in both considered scenarios.

Introduction

Nitrogen is an essential element to all microorganisms. In the case of *Escherichia coli* (*E. coli*), nitrogen is coupled to the carbon metabolism by the Krebs cycle, where the alpha-ketoglutarate is used to produce glutamate and glutamine which are the fundamental compounds to synthesize all other amino acids and proteins [1, 2].

In several microorganisms with industrial applications, nitrogen-limited batch or continuous microbiological cultures allow the control of the cell growth by maintaining a sub-optimal nitrogen level and prevent the cells from being starved and to stop growing [3].

For example, nitrogen limitation has showed to be a relevant condition to promote efficient neutral lipids accumulation in microalgae or increase the hydrogen rate production in photobacteria [4]. Other groups have also demonstrated that *Saccharomyces cerevisiae* increases ethanol yield under nitrogen limitation [5].

Despite the substrate concentration, feed flow rate and carbon bioavailability are well-known relevant issues that affect the microorganism metabolism. Carbon-to-nitrogen ratio (CNR) in the microorganism's culture media has started to be considered also as a critical aspect that can modify entirely the microorganism behavior [6].

In particular, aerobic and anaerobic cultures *E. coli* where the nitrogen source is ammonia (NH_4) are characterized by

✉ I. Chairez
isaac_chairez@yahoo.com

M. Rios-Lozano
mm.rios.lozano@gmail.com

[1] SEPI-UPIBI, Instituto Politécnico Nacional, Mexico, DF, Mexico

[2] Department of Bioprocesses, UPIBI, Instituto Politécnico Nacional, Mexico, DF, Mexico

the biomass growth with the corresponding carbon dioxide (CO_2) and formation of byproducts such as acetate, formate, lactate, ethanol, among others. However, in aerobic cultures, as soon as the nitrogen source is completely consumed, the microorganism growth is stopped but the remainder cells continue consuming glucose to produce CO_2 and water. On the other hand, in anaerobic conditions, the metabolism is redirected to produce only byproducts such as acetate, formate, lactate and ethanol.

Similar conditions (with a different distribution of byproducts) have been observed in some other microorganisms such as *Salmonella typhimurium* [7], *Saccharomyces cerevisiae* [8], etc.

The simplest model to describe growth of a microorganism limited by nitrogen is the Droop model. This model assumes that the growth rate depends on the intracellular concentration of nitrogen. More accurate models have been proposed to deal with the coupling between nitrogen and carbon assimilation under several conditions of light radiation [9–11].

However, the complete understanding of CNR effect on microorganism metabolite and genetic response may consume long periods of experimental procedures and remarkable amounts of resources. In this sense, mathematical modeling may play a key role on simplifying the conceptual study on the CNR relevance for each particular microorganism as well as on saving time and resources.

The model complexity must result from a trade-off between realism, in order to accurately represent the key variables of the process, and simplicity so that it can be mathematically tractable and suitable for calibration and to solve control and optimization problems [12].

Even more important is the concept that any mathematical model can be considered useless if it is not well characterized in regard of the particular microorganisms analyzed. Therefore, a detailed kinetic study and the associated parametric identification scheme are mandatory to characterize and validate the model. If this set of tasks can be successfully solved, then prediction of microorganisms behavior and optimization analysis can be easily proposed without important resource investments. There are many examples where some application of well-characterized models have been key elements on improving metabolites productiveness, feeding strategies, scale-up designs and control methods designs.

The main objective of this work is to obtain a parametric characterization of a simplified dynamical model able to predict biomass and metabolites productivity under nitrogen stress. The model was obtained considering the following facts:

- Biomass growth depends on both nitrogen and glucose.
- There is a proportional time-invariant relationship between carbon and nitrogen consumption rates.

- Byproducts generation is closely related to the biomass growth.
- Byproducts formation is related to the biomass accumulation.
- Dilution rate is considered constant.

The model is developed on the basis of experiments carried out under various nitrogen conditions (replete and starvation) with the *E. coli* as testing microorganism under aerobic conditions. This article also presents a novel parametric identification scheme to characterize the model under the different conditions analyzed in this study. This parametric identifier uses the sequential combination of several least mean square parametric identifier.

Mathematical model of microorganisms culture under nitrogen limitation

According to [1], nitrogen limitation condition in microbiological reactors can be modeled with the application of a modified specific growth rate. The mathematical model proposed in this study was proposed to support an optimization strategy and to guide the trade-off between growth and nitrogen effects on metabolites accumulation.

The proposed model must keep complexity at a minimal level to be mathematically tractable. Therefore, the number of variables was limited to the most important ones: biomass growth, substrate consumption and main byproducts accumulation. The model was designed to consider the relationship between all the above-mentioned variables.

This study focuses on the growth of *E. coli*, whose biomass, in terms of organic carbon, is denoted as $X(\text{g/L})$. This growth was supported by the injection of substrate denoted by $S(\text{g/L})$. Metabolites produced by *E. coli* were represented as $P_j(\text{g/L})$ with $j = 1, \ldots, N$.

In this study, two different scenarios were considered, the first one considers *E. coli* cells limited by a CNR source and a second one where this limitation was not longer considered with the corresponding increasing of CNR. In line with [13], the assumption on organic carbon that can be split into functional and storage pools is still holding. Despite the scenario considered to analyze the CNR effect on microorganism growth, compartmental method was the theoretical basement to develop the model.

The functional compartment (*f*) includes the biosynthetic apparatus (proteins and nucleic acids) and the structural material (membranes mainly made of glycolipids and phospholipids). In several microorganisms, nutrient uptake and biomass growth are known to be uncoupled processes for microalgae [14, 15] leading thus to variations in the internal quota of nutrient. However, this is not the

case for *E. coli*. Therefore, the biomass growth rate should include both effects simultaneously.

The model was based on the usual continuous stirred tank reactor model with a two-factor specific growth reaction rate [16–18]. This function was constructed as function of both carbon and nitrogen sources. In addition, the model considered the consumption of some key byproducts once the nitrogen or the substrate was completely consumed. This fact was modeled as a hybrid system considering a reference value N^* that can be identified by experimental analysis. Also, the model that considers the fact described above can be characterized by the following set of ordinary differential equations:

$$\frac{\mathrm{d}}{\mathrm{d}t}C(t) = F(C(t), u(t)) + \chi(N(t))F_N(C(t)), \qquad (1)$$

where $C = [X, S, P_1, \ldots, P_N]^\top$ and the vector field F satisfies:

$$F(C(t), u(t)) = \begin{bmatrix} \mu(X, S(t))X(t) - D(t)X(t) \\ D(t)(u(t) - S(t)) - \rho(S)X(t) \\ \mu_{P,1}X(t) \\ \vdots \\ \mu_{P,N}X(t) \end{bmatrix} \qquad (2)$$

with $N(t) = \alpha S(t)$. The time varying parameters $\rho(s(t))$ and $\mu(Q_N(t))$ are:

$$\rho(S(t)) = \rho_m \frac{S(t)}{S(t) + K_S}$$

$$\mu(S(t), N(t)) = \bar{\mu}\left(\frac{S(t)}{K_S + S(t)}\right)\left(\frac{N(t)}{K_N + N(t)}\right)$$

The biomass concentration is denoted as $X(\mathrm{g/L})$, the substrate concentration is denoted by $S(\mathrm{g/L})$ and the variation of the different products concentration is denoted by $P_i(\mathrm{g/L})$. The substrate uptake rate is represented as $\rho(1/\mathrm{h})$, while $\mu(1/\mathrm{h})$ is the specific growth rate and $D(1/\mathrm{h})$ is the constant dilution rate calculated as $D = Q_{\mathrm{in}}/V$ where $Q_{\mathrm{in}}, (\mathrm{L/h})$ and V, L are the input flow of external substrate and volume in the reactor, correspondingly.

The vector $F_N(C(t))$ presented in (2) characterizes the effect of substrate (either glucose or nitrogen) on the reaction dynamics. Indeed, this section models the utilization of organic acids as carbon source to keep the biomass growth continuing. Simultaneously, this part of the model highlights the effect of nitrogen limitation condition. In particular, this effect was evidenced in ethanol dynamics. This condition has been observed in some studies, but it has never been modeled before. The vector field $F_N(C(t))$ satisfies

$$F_N(C) = \begin{bmatrix} \mu_{N,1}P_1 + \mu_{N,2}P_2 \\ 0 \\ -\bar{\mu}_{P,1}X \\ \vdots \\ \mu_{P,N}X \end{bmatrix} \qquad (3)$$

This term has been introduced in the model (1) to justify the evidence of byproducts consumption as a secondary substrate. In [19], an initial substrate formed by glucose (50 g/L) and ammonia (1.0 g/L) evidenced the consumption of organic acids produced by the fermentation process. This fact was explained by the fastest complete consumption of nitrogen source that reduces the microorganism growing. Therefore, despite glucose being still consumed after nitrogen source was entirely consumed, lactate and acetate are used as substrate to satisfy the pyruvate and acetyl-coenzyme A demands which serve as key intermediates in many different metabolic mechanisms. The function χ serves to indicate when the alternative substrate sources should be used depending on the nitrogen presence on the medium. This term was used to introduce the hybrid nature of metabolism when nitrogen was consumed. Then

$$\chi(N) = \begin{cases} 1 & \text{if} \quad N \geq N^* \\ 0 & \text{if} \quad N < N^* \end{cases}, \qquad (4)$$

where N^* is the minimum nitrogen concentration needed to keep glucose as the main substrate for the microorganism.

Parametric identification algorithm

Model generalization

The model presented in (1) is composed by a set of equations formed by aggregations of rational functions depending on its states. The equivalent and simplified representation can be reorganized as a sum of two rational functions. The first one depended on the uncertain parameters included in the model and the second one did not. Therefore, each equation introduced in the model (1) can be generalized as follows:

$$\frac{\mathrm{d}C_i(t)}{\mathrm{d}t} = \frac{P_{1,i}(C(t))^\top a_i + N_{1,i}(C(t))}{P_{2,i}(C(t))^\top b_i + N_{2,i}(C(t))} + P_{3,i}(C(t)), \qquad (5)$$

where $P_{1,i}$ and $P_{2,i}$ are nonlinear vectors formed with polynomials of variables involved in model (2). The polynomial $P_{3,i}$ represents the parameter-independent terms that usually appears in biotechnological models. The variable C_i represents the ith state of (2). The vectors a_i and b_i are formed by the uncertain parameters of the systems presented in (2).

Based on the representation (5), one can get an equivalent representation such as

$$Y_i(T) = \Phi_i(T)^\top \Theta_i, \tag{9}$$

where

$$Y_i(T) = \int_0^T N_{1,i}(C(t))\mathrm{d}t - N_{2,i}(C(T))C_i(T)$$
$$+ \int_0^T \frac{\mathrm{d}N_{2,i}(C(t))}{\mathrm{d}t} C_i(t)\mathrm{d}t - \int_0^T P_{3,i}(C(t))N_{2,i}(C(t))\mathrm{d}t$$

$$\Phi_i(T) = \begin{bmatrix} -\int_0^T P_{1,i}(C(t))\mathrm{d}t \\ P_{2,i}(C(T))C_i(T) - \int_0^T \left[\frac{\mathrm{d}P_{2,i}(C(t))}{\mathrm{d}t} C_i(t) - P_{3,i}(C(t))P_{2,i}(C(t)) \right]\mathrm{d}t \end{bmatrix} \tag{10}$$

$$\Theta_i = \begin{bmatrix} a_i^\top & b_i^\top \end{bmatrix}^\top$$

$$\int_0^T \frac{\mathrm{d}C_i(t)}{\mathrm{d}t} P_{2,i}(C(t))^\top b_i \mathrm{d}t + \int_0^T N_{2,i}(C(t)) \frac{\mathrm{d}C_i(t)}{\mathrm{d}t} \mathrm{d}t$$
$$- \int_0^T P_{3,i}(C(t))[N_{2,i}(C(t)) + P_{2,i}(C(t))^\top b_i]\mathrm{d}t$$
$$= \int_0^T [P_{1,i}(C(t))^\top a_i + N_{1,i}(C(t))]\mathrm{d}t \tag{6}$$

A straightforward integration-by-parts of the left-hand side part of the previous equation leads to

$$P_{2,i}(C(T))^\top C_i(T)b_i - \int_0^T \frac{\mathrm{d}P_{2,i}(C(t))^\top}{\mathrm{d}t} C_i(t)\mathrm{d}t b_i$$

$$+ N_{2,i}(C(T))C_i(T) - \int_0^T \frac{\mathrm{d}N_{2,i}(C(t))}{\mathrm{d}t} C_i(t)\mathrm{d}t$$

$$- \int_0^T P_{3,i}(C(t))[N_{2,i}(C(t)) + P_{2,i}(C(t))^\top b_i]\mathrm{d}t \tag{7}$$

$$= \int_0^T P_{1,i}(C(t))^\top \mathrm{d}t a_i + \int_0^T N_{1,i}(C(t))\mathrm{d}t,$$

where the derivatives of $P_{2,i}$ and $N_{2,i}$ can be calculated as follows:

$$\frac{\mathrm{d}P_{2,i}(C(t))}{\mathrm{d}t} = P'_{2,i}(C)F(C(t))$$

$$\frac{\mathrm{d}N_{2,i}(C(t))}{\mathrm{d}t} = N'_{2,i}(C)F(C(t)) \tag{8}$$

$$P'_{2,i}(C) = \frac{\mathrm{d}P_{2,i}(C)}{\mathrm{d}C}$$

$$N'_{2,i}(C) = \frac{\mathrm{d}N_{2,i}(C)}{\mathrm{d}C}$$

Certainly, the previous structure can be represented as follows:

LMS step-by-step identification method

Based on the regular technique of the well-known least mean square method (LMS), the parametric identification problem presented in (9) can be solved as follows:

$$\Theta_i^* = \left[\sum_{k=0}^N \Phi_{i,k}(T)\Phi_{i,k}(T)^\top \right]^{-1} \left[\sum_{k=0}^N Y_{i,k}(T)\Phi_{i,k}(T) \right], \tag{11}$$

where the index k is used to represent the number of experiments considered in the study while N is the total number of experiments.

This methodology was followed to recover the set of parameters included in the model (2). The procedure used in this study was the following:

1. The parameters ρ_m and K_S are calculated from the second equation proposed in (2) with the following selection of polynomials: $N_{1,2} = 0$, $N_{2,2} = S$, $P_{1,2} = SX$, $P_{2,2} = 1$ and $P_{3,2} = D(u - S)$. The result of this process yields the estimates of $\hat{\rho}_m$ and $\hat{K}_S$.

2. The parameter $\hat{K}_s$ obtained in the previous step is used to estimate the parameters $\bar{\mu}_m$ and K_N are calculated using the first equation proposed in (2) with the following selection of polynomials: $N_{1,1} = 0$, $N_{2,1} = (\hat{K}_S + S)N$, $P_{1,1} = SN$, $P_{2,1} = (\hat{K}_S + S)$ and $P_{3,1} = DX$. The result of this process yields the estimates of $\hat{\rho}_m$ and $\hat{K}_S$.

3. The set of parameters $\mu_{P,i}$ are calculated directly from the equations fourth to Nth in (2) with the following selection of polynomials: $N_{1,3} = 0$, $N_{2,3} = 1$, $P_{1,3} = X$, $P_{2,3} = 0$ and $P_{3,3} = 0$.

Evaluation and identifications

A set of three different measures was computed from the identification and validation experiments in order to evaluate the goodness of fit and model prediction ability, respectively. Therefore, the information obtained in the three experiments was used to validate the model. Three sequences of validation process were done. In each one of these validation tests, the experimental and simulated information of two sets were averaged. This set of information was injected to the parametric identification method. After that, the remainder (the one left out) was evaluated to validate the model. The error obtained in the identified parameter within each analysis was averaged. This final error was reported to characterize the quality of the method proposed in this study.

Experimental strategy

A set of aerobic experiments was executed in triplicate. These experiments were carried out with two different C/N ratio. Under these conditions, biomass, substrate and some metabolites were analyzed. These elements were used to characterize the E. coli growth and its secondary metabolic evolution.

These data were used to characterize the effect of C/N ratio by parametric identification methods. Based on the variations of the parameters involved within the model presented in (2), the nitrogen limitation over the E. coli growth was discussed.

Materials and methods

Biological and chemical materials

The bacterial strain used to perform all the experiments is E. coli K-12. Microorganisms inoculation was prepared by a preliminary culture of 12 h at 37 °C and 200 rpm in controlled incubator.

This inoculum was cultured in several seed lab-scale baffled reactors with a volume of 0.5 L. The fermentation medium was based on M9 commercial solution (3.0 g/L of KH_2PO_4, 6.0 g/L of Na_2HPO_4, 0.5 g/L of NaCl, 1.0 g/L of NH_4Cl, 0.49 g/L of $MgSO_4 7H_2O$ and 0.11 g/L of $CaCl_2$) supplemented with glucose (2.0 g/L). Inoculation process used 200.0 mL of two different seed reactors (100.0 mL from each one).

All solvents and reagents were HPLC analytic grade. Glucose, acetic acid, lactic acid and ethanol were purchased from Sigma-Aldrich (Sigma-Aldrich, USA). Concentrated sulfuric acid was purchased from Fermont (Mexico). Standard solutions were used to determine the variation of substrate and byproducts during the fermentation. Primary stock solution of glucose, acetic acid, lactic acid and ethanol (10 g/L) was prepared in distilled water, and stored at 4 °C. Intermediate working solutions (0.01, 0.05, 0.1, 0.2, 0.5, 1 and 2 g/L) were obtained through dilutions of this primary stock solution with distilled water and filtered through a 0.22 μm filter before the injection into the chromatographic column.

Fermentation process

All fermentation experiments were evaluated in 3.0-L Bioflo reactors. Culture media for this part of the study was M9 commercial solution supplemented with glucose (10.0 and 50.0 g/L) and yeast extract (3.0 g/L). Initial pH was adjusted to 7.0 using either NaOH 2.0 N or H_2SO_4 2.0 N when necessary. Reactor temperature was controlled to the constant value of 37 °C by a water bath. Dissolved oxygen was fixed (by an external controller) at 20 % above the air saturation level. Air inject velocity was fixed to 0.5 vvm.

Samples were withdrawn from the reactor during 24.0 h at fixed intervals of 2.0 h. The sample volume was 20.0 mL. These samples were centrifuged in 50.0-mL Falcon tubes at 6000.0 rpm, 4.0 °C during 15.0 min. Cells separated by this process were diluted in 20.0 mL of distilled water. This process was used to obtain the dry weight of samples.

The CNR effect on E. coli under aerobic conditions was evaluated by running two different set of reactions where the initial glucose concentration was 50.0 g/L, while ammonia concentration was 1.0 g/L and in the second set, the glucose concentration was 10.0 g/L with the same concentration of the nitrogen source. Experiments were executed in triplicate.

Experimental methods

Optical density analysis

Microorganisms growth was determined by the regular optical density method measured at 600 nm by UV–Vis spectrometer. A 3.0-mL sample was withdrawn from the reactor to complete this analysis. The sample was diluted until reaching the adequate absorbency value within the 0.1–1.0 range. Dilution ratios were 1:3, 1:5 and 1:10 depending on the fermentation time.

Dry weight analysis

Extra 5.0-mL samples were dried in oven with fixed temperature of 60 °C. This process was executed for a period of 48 h. This condition ensured a constant weight for the dried sample.

HPLC analysis

HPLC (RI detector, Smartline, KNAUER, Germany) analysis was proposed to characterize the metabolite time evolution throughout the fermentation. A set of operation conditions was proposed to obtain the alcohol and organic acids variation, respectively. A 2.0-mL filtered (0.22 μm membrane) sample was diluted 1:5 with distilled water previous to HPLC analysis (Table 1). The mobile phase was 0.005 N of H_2SO_4.

Ammonia detection method

Phenol-hypochlorite method was used to characterize the ammonia ion. NH_4Cl and $(NH_4)_2SO_4$ were used as standard compounds. The method was executed using the supernatant of samples taken periodically from the bioreactor. Each sample was diluted 1:10. A volume of 20μL was mixed with 5 mL of solution A during 5 min of continuous agitation. Then 5 mL of solution B was added with continuous agitation for 5 more minutes. The mixed samples were incubated for 30 min. The incubated samples were measured by the spectrophotometer at 625 nm. Solution A was prepared by 10 g/L of phenol and 50 mg/L of sodium nitroprusside while solution B was prepared by 5 g/L of NaOH and 8.4 mL/L of sodium hypochlorite.

Evaluation of identification method

The method proposed here was evaluated under two different scenarios. The first one considers the identification process based on a set of simulations of (2) while the second one used the real information obtained by real experiments. Next section describes the results obtained when the model (2) was used as data generator.

Simulated system

In this part of the evaluation, the model (2) was simulated with the parameters presented in the Table 2. These parameters were estimated in different scientific results regarding the estimation of parameters [1]. Their values were adjusted to reproduce the general behavior of biomass, substrate, lactate, acetate and ethanol collected at the experimental period. Under the selected set of parameters, the simulated microorganism growing was modulated by the CNR.

The parameter identification method was simulated under the following conditions: data generation was obtained in Matlab using Simulink scheme with a Runge–Kutta integration method with integration step of 0.001 s. The set of parameters obtained by the application of the identification method is shown in Table 3. In this case, the relative error between the actual and estimated parameters was less than 10 %. This condition can be considered

Table 2 Parameters used in the simulation of the mathematical model

Parameter	Value	Units
Q^{in}	0.000	L/h
V	3.000	L
$\bar{\mu}$	3.000	1/h
ρ_m	1.320	1/h
K_S	2.500	g/L
K_N	3.500	g/L
$\mu_{P,1}$	0.050	1/h
$\mu_{P,2}$	0.160	1/h
$\mu_{P,3}$	0.009	1/h
$\mu_{N,1}$	0.100	1/h
$\mu_{N,2}$	0.150	1/h
$\bar{\mu}_{P,1}$	0.250	1/h
$\bar{\mu}_{P,2}$	0.210	1/h
$\bar{\mu}_{P,3}$	0.010	1/h

Table 1 HPLC conditions for experiments

Condition	Value
Column	Rezex Roa Org Aci H+ (8 %), Phenomenex, USA
Dimensions	300 × 7.8 mm
Oven temperature	60 °C
Flow	0.6 mL/min
Carrier phase	0.005 N H_2SO_4
Detector	Refraction index
Injection volume	20μL
Analysis period	30 min

Table 3 Estimated parameters in the model and its relative error with respect to the actual values

Parameter	Value	Units	Error (%)
Q^{in}	0.000	L/h	0.0
V	3.000	L	0.0
$\bar{\mu}$	3.190	1/h	6.7
ρ_m	1.430	1/h	8.3
K_S	2.673	g/L	6.8
K_N	3.345	g/L	4.4
$\mu_{P,1}$	0.047	1/h	6.0
$\mu_{P,2}$	0.175	1/h	9.3
$\mu_{P,3}$	0.009	1/h	0.0
$\mu_{N,1}$	0.109	1/h	9.0
$\mu_{N,2}$	0.156	1/h	4.0
$\bar{\mu}_{P,1}$	0.264	1/h	5.6
$\bar{\mu}_{P,2}$	0.224	1/h	6.7
$\bar{\mu}_{P,3}$	0.011	1/h	10.0

acceptable when the nature of the system is taken into account.

The model was simulated in a second round using the estimated parameters. The relative error between both trajectories was evaluated by comparing the trajectories of both sets of states.

Figure 1 shows the comparison between the states obtained by simulating the model with the original parameters as well as the estimated ones. In all cases, solid and dashed lines were used to represent the original states. Dotted lines were used to represent the simulated states when the estimated parameters were used. The only relevant difference was obtained when the ethanol concentrations were compared. The subfigures placed at the left (Fig. 1a–c) show the results of simulation when CNR was low. On the other hand, the subfigures located at the right contain the information of states obtained from the model simulated under the conditions of high CNR (Fig. 1d–f). One may notice the significant differences between trajectories obtained when CNR was varied.

Figure 1a depicts the comparison of both biomass and substrate concentrations with their respective variation observed as solution of the modeling process when no nitrogen limitation was forced in the reactor. Figure 1d describes the corresponding variation of biomass and substrate concentrations but this time the nitrogen limitation was simulated. In both cases, with and without nitrogen limitation the approximation achieved by the model developed in this study.

Figure 1b, e shows the variation of both ethanol and lactic acid. This time the correspondence between the

estimated values by the model and the ethanol variations was not so efficient. This fact is justified because the high rate of ethanol consumption cannot be modeled without making artificial assumptions on the metabolic response of *E. coli*.

Figure 1c, f shows the acetate variation in both cases of nitrogen availability considered in this study. The evident variations between these two figures demonstrate how the inability of *E. coli* to continue using glucose as substrate forces acetate consumption. This can be confirmed in simulation considering the times when the nitrogen is completely consumed (7 and 6 s with and without nitrogen limitation). The nitrogen consumption was modeled as explained in Eq. (2).

Experimental results

Biomass growth as well as substrate consumption are depicted in Fig. 2a, d. If no nitrogen limitation was the condition in the reactor (CNR 5:1), glucose is used as main carbon source (Fig. 2a). Indeed, substrate is eliminated after 6.21 h of reaction. Nitrogen source remained in the reactor with a final concentration of 0.2 g/L. Final biomass concentration reached a 4.53 g/L measured as dried weight. The biomass/substrate yield was 0.45.

In the case of the 1:1 CNR ratio (Fig. 2b), ammonia was not detected in the reactor after 6.0 h. However, the biomass concentration at that moment was 6.4 g/L (35 % higher than the case when nitrogen was not the limiting reagent). Nevertheless, after nitrogen was eliminated completely from the reactor, the biomass concentration decreased continuously until reaching 5.1 g/L. Moreover, the glucose consumption velocity changed from its expected exponential form to an almost linear condition.

Figures 2, 3 and 4 show the trajectories of the model simulated with the parameters presented in Table 3 that corresponds to both CNR. These figures show the time evolution of biomass, substrate, acetate, ethanol and lactate when CNR ratio was 1:1 and 5:1. The parameter estimation method was also executed when both CNR ratios were considered in the reaction (data are shown when CNR was 5:1). In both cases, the simulated model using the parameters obtained in this study yields to a correct correspondence between estimated and experimental concentrations of all compounds. Once more, in all cases, solid and dashed lines were used to represent the original states. Dotted lines were used to represent the simulated states when the estimated parameters were used.

When the 5:1 CNR was evaluated, acetate was also used as carbon source after glucose disappeared (Fig. 4a) and lactate was consumed during the first 1.5 h of the reaction (Fig. 3a). Biomass concentration did not diminish because acetate was also used as carbon source (Fig. 2a).
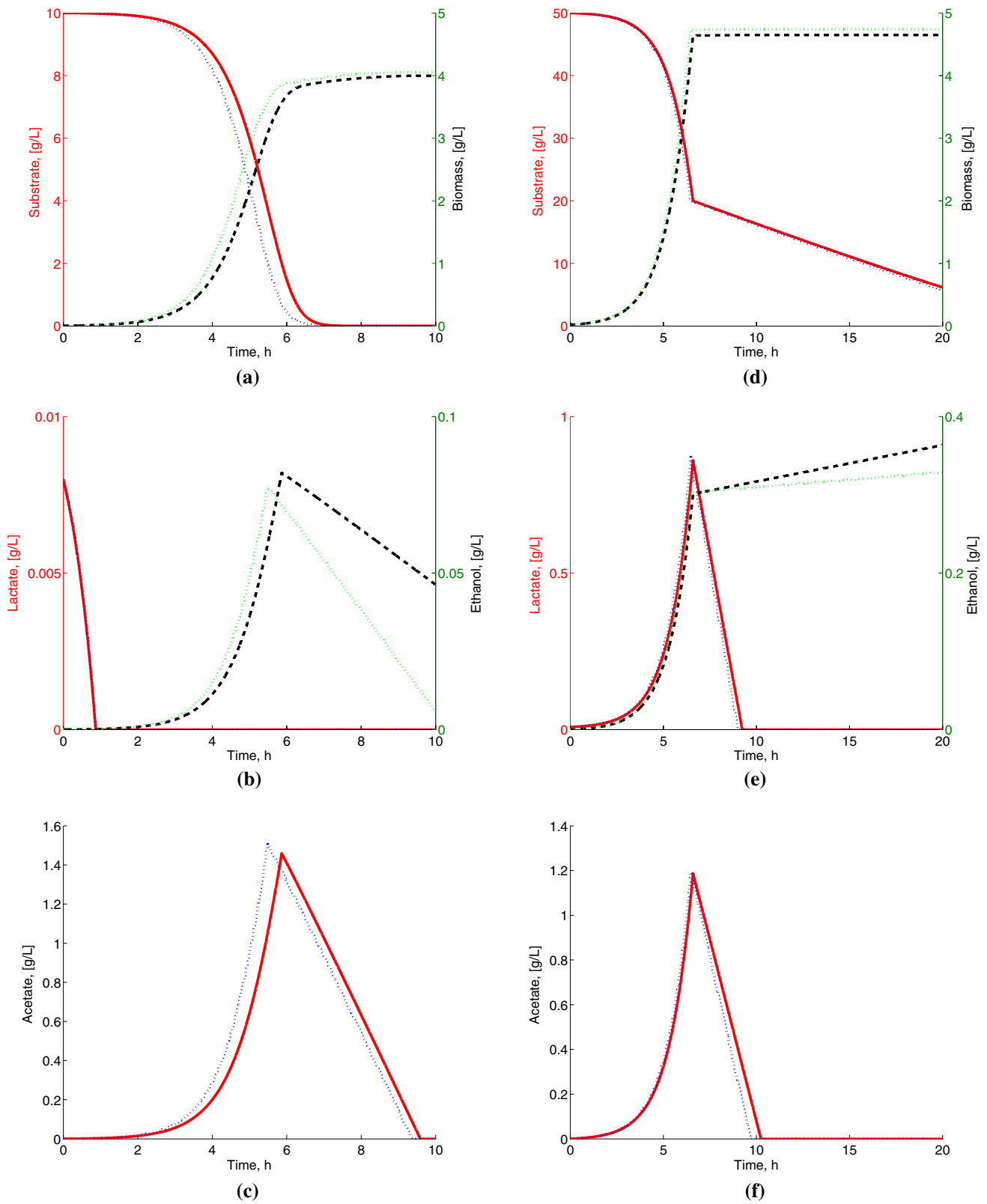
Fig. 1 Evolution of the states included in the Eq. (2) when simulated with the estimated parameters presented in Table 4

Fig. 2 Comparison of both biomass and substrate evolution under two different CNR conditions was evaluated: 5 to 1 (**a**) and 1 to 1 (**b**). Experimental results as well as states of model presented in Eq. (2) executed with estimated parameters are also compared
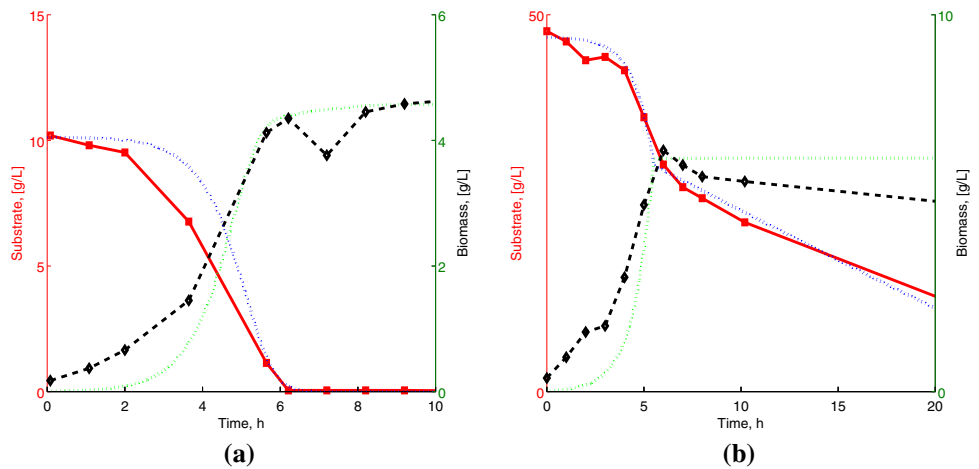

Fig. 3 Comparison of both lactate and ethanol evolution under two different CNR conditions was evaluated: 5 to 1 (**a**) and 1 to 1 (**b**). Experimental results as well as states of model presented in Eq. (2) executed with estimated parameters are also compared
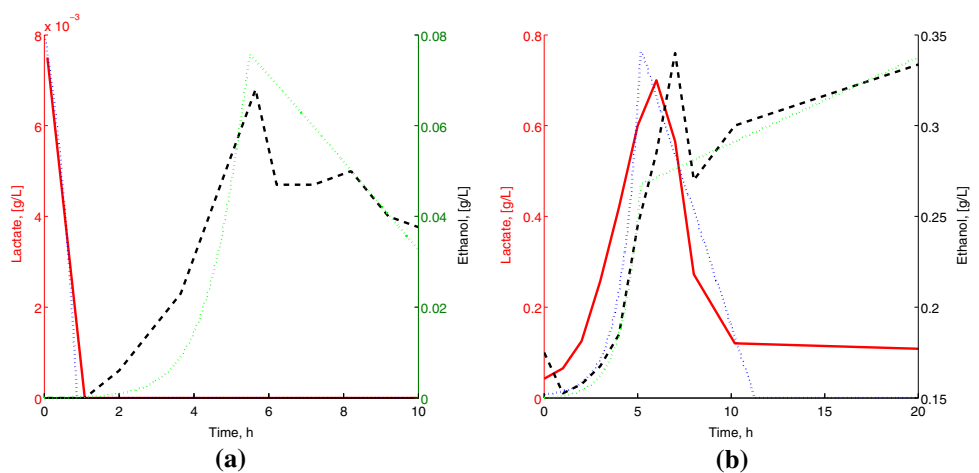

Fig. 4 Comparison of acetate evolution under two different CNR conditions was evaluated: 5 to 1 (**a**) and 1 to 1 (**b**). Experimental results as well as states of model presented in Eq. (2) executed with estimated parameters are also compared
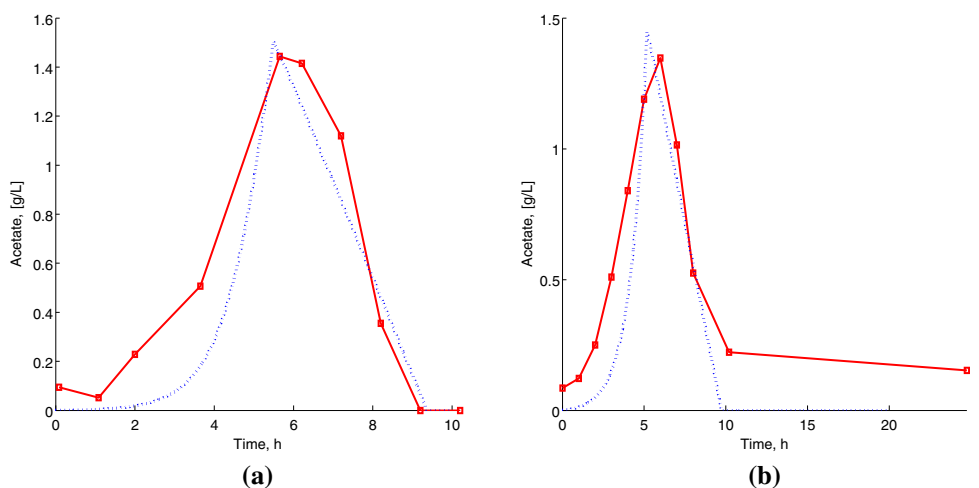
When the 1:1 CNR was evaluated, biomass followed the same pattern during the first 5 h of culture. After the nitrogen was detected in the reactor (below the limiting detection), the biomass concentration decreased because the main substrate was not usable any longer (Fig. 2b). Lactate was accumulated during the first 6 h (before the nitrogen source was completely consumed). After that moment, this byproduct was used as an alternative carbon

Table 4 Estimated parameters obtained with the experimental information

Parameter	Value	Units
Q^{in}	0.000	L/h
V	3.000	L
$\bar{\mu}$	3.190	1/h
ρ_m	1.430	1/h
K_S	2.473	g/L
K_N	3.305	g/L
$\mu_{P,1}$	0.081	1/h
$\mu_{P,2}$	0.115	1/h
$\mu_{P,3}$	0.008	1/h
$\mu_{N,1}$	0.129	1/h
$\mu_{N,2}$	0.165	1/h
$\bar{\mu}_{P,1}$	0.284	1/h
$\bar{\mu}_{P,2}$	0.264	1/h
$\bar{\mu}_{P,3}$	0.059	1/h

source because it was consumed during the next 6 h (Fig. 3b). A similar condition was observed for the case of acetate (Fig. 4b) that also was consumed since the moment that nitrogen was no longer detected.

It is noticeable that in both CNR experiments, acetate was preferably used as substituting carbon source of glucose. This fact was confirmed indirectly by the velocity consumption showed in both conditions (lower and higher CNR). Then, acetate and lactate were also used as carbon sources considering that they both were consumed after the nitrogen source was not detected. Nevertheless, glucose was also consumed during that period of the reaction but less efficiently compared to the case when nitrogen was still detected in the reactor. So, the presence of nitrogen can be characterized as regulator of the substrate consumption efficiency.

The final byproduct, ethanol, was accumulated in both cases (lower and higher CNR) (Fig. 3). Nevertheless, when nitrogen was not limited, ethanol decreased after glucose was consumed (Fig. 3a). One feasible explanation regards to the evaporation condition after it was not longer produced and considering the reactor temperature which is slightly above the evaporation temperature of the alcohol. When nitrogen was eliminated from the reactor in the case of the smaller CNR, ethanol was accumulated slower after the nitrogen was consumed, but still its concentration continued accumulating (Fig. 3b).

This part of the section shows the estimated parameters obtained when experimental studies were conducted under predefined different CNR. The similarities between trajectories obtained as result of the experimental information as well as the simulated model with the estimated parameters represent a promising condition to validate the model. However, there are several additional experiments where some other experimental conditions must be changed in

order to verify the generalization capacity of the model proposed in this study (Fig. 4).

The mean square error for the estimation process was calculated for evidencing the exact convergence of the parameter identification method proposed in this study. Even when the values of this figure seem to be very high, comparing with the values of the states presented in Fig. 4 are relatively low. The similarities between experimental information and the trajectories of the model obtained with the parameters recovered by the algorithm proposed in this study, suggest that the solution proposed here can be used to characterize the CNR effect on *E. coli*. Eventually, this tool can be modified to include the effect of some other substrates.

Conclusions

This paper introduces a parametric algorithm to characterize the effect of CNR on the growth of *E. coli*. The algorithm consisted of a novel strategy based on the least mean square method applied over the characteristic model of batch aerobic reaction. The identification method showed significant differences between the parameter values associated to the biomass growth of *E. coli*. The parameter identification method was tested using either numerical or experimental information. In the case of numerical information, the maximum relative error between the actual and estimated parameters was less than 10.0 %. In both cases, the model was simulated with the estimated parameters. The mean square error was analyzed yielding to justify the inclusion of the parameter identification algorithm to characterize the CNR using experimental data. The identification maximum error of 5 % is considered acceptable when they are compared with similar results obtained in similar studies regarding parameter estimation of bioprocess systems. Finally, the parameters estimated by the algorithm proposed in this study helped to characterize the effect of CNR ratio on the growth of *E. coli*. A natural further step on this investigation is to evaluate the effectiveness of the method when the reaction could be executed under anaerobic conditions. Additionally, the CNR can be also used as a regulatory factor to optimize (increasing the yields) the industrial production of several *E. coli*'s secondary metabolites.

References

1. van Heeswijk WC, Westerhoff H, Boogerd FC (2013) Nitrogen assimilation in *Escherichia coli*: putting molecular data into a systems perspective. Microbiol Mol Biol Rev 77(4):628–695

2. Reitzer L (2003) Nitrogen assimilation and global regulation in *Escherichia coli*. Annu Rev Microbiol 57:155–176
3. Falkowski PG, Raven JA (2007) Aquatic photosynthesis. PaperBack
4. Zhang L, He M, Liu J (2014) The enhancement mechanism of hydrogen photoproduction in chlorella protothecoides under nitrogen limitation and sulfur deprivation. Int J Hydrogen Energy 39(17):89698976
5. Niessen J, Harnisch F, Rosenbaum M, Schroder U, Scholz F (2006) Heat treated soil as convenient and versatile source of bacterial communities for microbial electricity generation. Electrochem Commun 8:869–873
6. Baez A, Cho KM, Liao JC (2011) High-flux isobutanol production using engineered *Escherichia coli*: a bioreactor study with in situ product removal. Appl Microbiol Biotechnol 90(5):1681–1690
7. Ikeda M, Arai K, Masai H (1996) Ctbp1/rbp1, a *Saccharomyces cerevisiae* protein which binds to t-rich single-stranded DNA containing the 11-bp core sequence of autonomously replicating sequence, is a poly(deoxypyrimidine)-binding protein. Eur J Biochem 238(1):38–47
8. Larsson C, Nilsson A, Blomberg A, Gustafsson L (1997) Glycolytic flux is conditionally correlated with ATP concentration in *Saccharomyces cerevisiae*: a chemostat study under carbon- or nitrogen-limiting conditions. J Bacteriol 179(23):7243–7250
9. Geider RJ, MacIntyre HL, Kana TM (1998) A dynamic regulatory model of phytoplanktonic acclimation to light, nutrients, and temperature. Limnol Oceanogr 43(4):679–694
10. Faugeras B, Bernard O, Sciandra A, Levy M (2004) A mechanistic modelling and data assimilation approach to estimate the carbon/chlorophyll and carbon/nitrogen ratios in a coupled hydrodynamical-biological model. Nonlinear Process Geophys 11:515–533
11. Pahlow M, Dietze H, Oschlies A (2013) Optimality-based model of phytoplankton growth and diazotrophy. Mar Ecol Prog Ser 489:1–16
12. Bernard O, Queinnec I (2008) Dynamic models of biochemical processes: properties of the models. Hermes Science, Paris
13. Ross ON, Geider RJ (2009) New cell-based model of photosynthesis and photo-acclimation: accumulation and mobilisation of energy reserves in phytoplankton. Mar Ecol Prog Ser 383:53–71
14. Chisti Y (2007) Biodiesel from microalgae. Biotechnol Adv 25:294–306
15. Christenson L, Sims R (2011) Production and harvesting of microalgae for wastewater treatment, biofuels, and bioproducts. Biotechnol Adv 25:686–702
16. Thamsiriroj T, Murphy JD (2011) Modelling mono-digestion of grass silage in a 2-stage CSTR anaerobic digester using ADM1. Bioresour Technol 102(2):948–959
17. Boe K, Angelidaki I (2009) Serial CSTR digester configuration for improving biogas production from manure. Water Res 43(1):166–172
18. Gibon-Fargeot AM, Celle-Couenne F, Hammouri H (2000) Cascade estimation design for CSTR models. Comput Chem Eng 24(11):2355–2566
19. El Mansi EMT, Holms WH (1989) Control of carbon flux to acetate excretion during growth of *Escherichia coli* in batch and continuous cultures. J Gen Microbiol 135(11):2875–2883